Design and Development of the Primary and Secondary Mirror Deployment Systems for the Cryogenic JWST

Paul Reynolds*, Charlie Atkinson* and Larry Gliman*

Abstract

With a 7-meter primary mirror (PM) aperture, the James Webb Space Telescope (Figure 1) will require structures that remain stable to levels on the order of 10 nanometers out of plane under dynamic and thermal loading while operating at cryogenic temperatures. Moreover, the JWST will be the first telescope in space to deploy primary and secondary mirrors. The resulting primary mirror (PM) aperture will not only be segmented, but will have hinge-lines and associated latches. The secondary mirror will be deployed with folding booms that latch to support it approximately 7 m away from the PM. This paper describes the design of the JWST Optical Telescope Element (OTE) structures and mechanisms, focusing primarily on the primary and secondary mirror deployment systems. It discusses the driving design requirements, how the resulting designs satisfy those requirements, and how the risk associated with these very large, stable, deployed structures was reduced through development and testing of the Development Optical Telescope Assembly (DOTA).

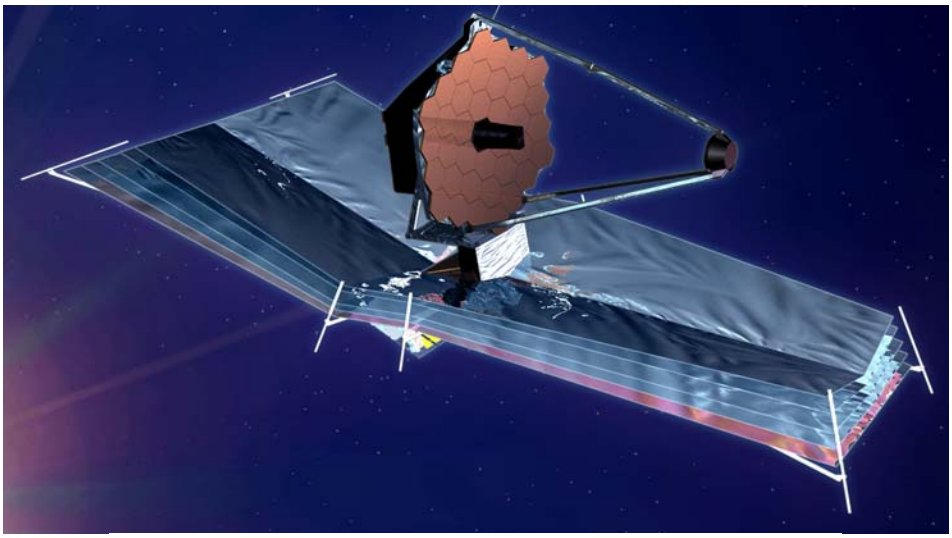

Figure 1. James Webb Space Telescope

Introduction

The James Webb Space Telescope (JWST) is a 7-m cryogenic telescope with near and mid-infrared instruments for imaging and spectroscopy. It will be used to help understand the shape and chemical composition of the universe, and the evolution of galaxies, stars and planets. The program held its Systems SRR in December of 2003, with PDR scheduled for 3/06, CDR in 3/07 and launch in 2011. NASA's Goddard Space Flight Center runs the JWST project out of Greenbelt, Maryland and is also responsible for delivering the Integrated Science Instrument Module (ISIM) to the observatory. Northrop Grumman Space Technologies (NGST) is the prime contractor and is teamed with: Ball Aerospace, who will provide the telescopes optics and wavefront sensing and control system, Kodak, who will integrate the optics onto the telescope structure assembly, and Alliant Techsystems, who will design and build the OTE's precision backplane structure and Secondary Mirror Support Structure (SMSS) struts. As the prime contractor, NGST has overall program responsibility and is responsible for the design and fabrication of

* Northrop Grumman Space Technology, Redondo Beach, CA

the OTE, spacecraft, and sunshield and the overall integration of the observatory. As part of NGST's responsibilities we are designing and building the deployment systems for the OTE. The OTE has 4 principal deployments: a tower deployment that thermally isolates the cryogenic telescope from the warm spacecraft and sunshield, two primary mirror wing deployments, and a secondary mirror deployment.

This paper will focus on the development of the deployment systems for the primary mirror wings and the secondary mirror. The discussion will center on some of the unique design challenges including deployment and operation at cryogenic temperatures, and the need for nanometer level stability over extended observations and after slewing from one target to the next. It will also discuss in detail the development and testing of the DOTA structures and mechanisms, how the DOTA designs relate to the JWST designs, and how the DOTA test results relate to the JWST requirements.

Requirements and Design Drivers

The JWST observatory will orbit the second Lagrangian point, L2, which is located 1.5 million kilometers from earth, in line with the earth and sun (Figure 2). The reason for this choice of orbit is the desire to passively cool the telescope to cryogenic temperatures with a deployable sunshield that blocks light from the Sun, Earth and Moon. The telescope needs to be at cryogenic temperatures to prevent it from emitting more radiation than the infrared light from faint and very distant objects.

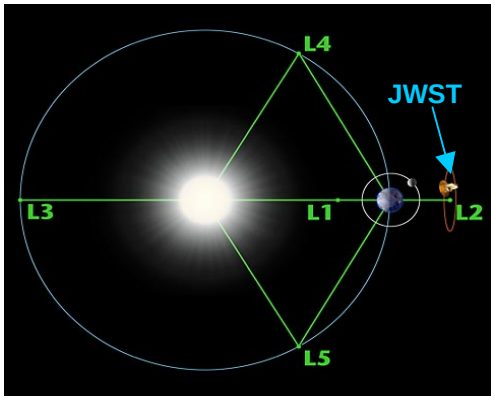

Figure 2. JWST Orbit Around L2

One of the primary drivers to shape the JWST architecture was the need to configure a large primary mirror that would stow along with its associated secondary mirror, instrument suite, sunshield, and spacecraft, within the volume provided by a medium Evolved Expendable Launch Vehicle (EELV). Essential to this objective was the need to keep deployments as low risk as possible and create optics support structures stable to nanometer levels.

Figure 3 shows the deployed observatory with some of its critical dimensions. The primary mirror is 7 m in diameter and the secondary mirror is 7.2 m forward of the primary mirror vertex. The sunshield, which passively cools the telescope, is approximately 25 m long by 10 m wide. A telescoping deployment tower extends 1.5m to separate the OTE from the spacecraft, resulting in a total observatory height of over 10m.

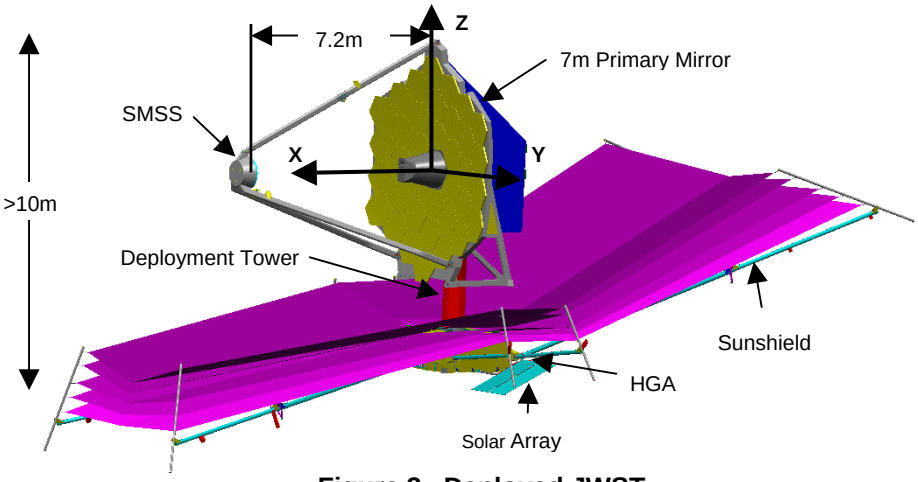

Figure 3. Deployed JWST

Since the EELV static envelope is 4.2 m in diameter, the primary mirror, secondary mirror, sunshield, solar arrays, radiator shades and High Gain Antenna (HGA) needed to be folded or compressed to fit within the allowable volume. The OTE to Spacecraft Deployment Tower raises the OTE off of its launch

lock attachment to the spacecraft and also provides thermal separation. Figure 4 shows the stowed observatory with the two wings and SMSS folded to provide clearance to the Atlas V static envelope.

The launch stiffness requirements for the observatory are specified in the EELV users guide. Based on the requirements and maturity of the design, the observatory is being designed to have a stowed natural frequency of 11 Hz. It must also be designed to survive the EELV launch loads listed in Table 1.

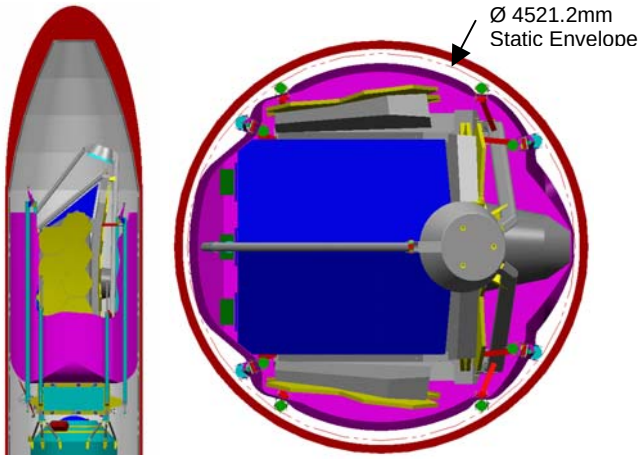

Figure 4. Stowed Observatory in Atlas V

Table 1. EELV Inertial Launch Loads

Case	Axial	Lateral		
Maximum Axial	2.0 ±5.5	2.0 at OTE/SV Interface	2.6 at OTE Top	Linear variation between
Maximum Lateral	2.0 ±2.60	3.5 at OTE/SV Interface	4.5 at OTE Top	Linear variation between

Once the observatory has separated from the launch vehicle, the solar arrays and radiator shades are deployed so the observatory can begin generating power. This is followed by the deployment of the HGA. The sunshield is deployed next and must deploy prior to the OTE since it cocoons the OTE when it is stowed. Next, the tower deploys the telescope away from the spacecraft and sunshield for thermal isolation. The planned deployment sequence has the SMSS deploying next, followed by the +Y and –Y primary mirror wings, though this order is not required.

Nominally, the tower, SMSS and wings deploy directly after the sunshield, while the telescope is still well above its cryogenic operating temperature. However, the OTE must be designed for any contingency including delays that could result in structure and mechanism temperatures as low as 30K prior to deployment. A combination of cryogenic deployment motors, heaters and careful selection of the mechanism materials will be used to make deployment at these very low temperatures possible.

Both the Primary Mirror Segment Assemblies (PMSA's) and the Secondary Mirror Assembly (SMA) have active control to correct for deployment errors or distortions that occur during cool down. However, the amount of allowable deployment error is limited by the wavefront sensing and control systems ability to capture an initial image so it can make its corrections. The deployment repeatability requirements are shown below in Table 2.

Table 2. Deployment Repeatability Requirements

JWST Requirement	**X Despace (mm)**	**Y Decenter (mm)**	**Z Decenter (mm)**	**Theta Z (arcmin)**
Primary Mirror Wings	1	0.1	0.1	1
Secondary Mirror	3	3	3	5

Once the OTE is deployed, the primary and secondary mirror support structures and mechanisms must remain stable to prevent degradation of telescope image quality and to eliminate the need for time-consuming adjustment of the adaptive optics. The thermal stability requirements of the primary mirror wing latches and SMSS (shown in Table 3) are provided in the form of allowable distortions during the worst case operational temperature swings. The sources of these distortions include non-zero CTE materials, variations in CTE within a material, manufacturing tolerances and thermal gradients across the structures and mechanisms.

Table 3. Thermal Stability Requirements

PM Latch Distortion Parameter	req't	units
Z translation (parallel to hinge line (HL))	0.05	μm dec
Y translation (perpendicular to HL)	0.1	μm dec
Piston of Mirror Segment	0.005	μm piston
Rotation about HL (Z)	0.01	μrad
Rotation perpendicular to HL (about Y)	0.0025	μrad
Gamma rotation(about X)	1	μrad

SM Motion Parameter	req't	units
Focus	1.34	□m
Translation	5	□m
Tip/Tilt	0.5	arcsec

In addition to errors caused by changes in the thermal environment, there are allocations for errors due to nano-lurching caused by stresses internal to the structures and mechanisms and/or on-orbit loading. The JWST image quality requirements allow for 20 nm of wavefront error (WFE) for these micro-dynamic events. Because of these requirements, the systems must be designed with micro-dynamics in mind and will be tested under operational load conditions to demonstrate stability within their allocation.

Disturbances from the spacecraft (e.g. reaction wheels) are attenuated by a 1-Hz isolator located at the base of the OTE deployment tower. Deployed natural frequency requirements have also been set for the OTE to further prevent the spacecraft disturbances from causing unacceptable motions of the primary mirror. These are referred to as line of sight (LOS) and WFE jitter requirements. The required natural frequencies for jitter are determined through integrated modeling using NASTRAN finite element math models in conjunction with Code V optical analysis models. Based on these models, the PM wings and SMSS must have deployed natural frequencies of 15 Hz and 7 Hz respectively.

The Design

Design Practices for Deployable Optics

When we began our mechanisms design, NASA Langley Research Center, with the help of JPL and the University of Colorado had recently published a study identifying guidelines for good design practices for micro dynamically stable deployable optics. Much of the design practices, however, had not been proven out in working designs. The approach NGST took for the PM and SMSS latch designs was to apply the published good design practices [1] that fit with our design approach, along with standard practices typically applied to mechanism design at NGST. Then an in-house system was developed to test the performance of the resulting hinge and latch designs.

Among the good design practices applied was to have kinematic (or quasi-kinematic) interfaces between optical components. One of the primary benefits we saw with a kinematic interface was the ability to preclude the development of unwanted interface loads (i.e., loads due to manufacturing and assembly tolerances and thermal loading due to cool-down), hence reducing the likelihood of friction-induced slippage. In addition, we believed using this type of interface in a deployment latch would result in good deployment repeatability. This is clearly demonstrated in the PM wing latch design.

Non-conforming contact geometries (i.e., point or line contacts) were used at the latching interfaces on the PM wing latches and for the mid-hinge of the SMSS. It is believed that this type of interface helps insure that the interface stress distribution is accurately known and prevents sensitivity to localized imperfections over large mating surfaces. However, in our applications we found that trying to use non-conforming contact geometries in a truly kinematic configuration resulted in unacceptably low stiffness.

Therefore, it was necessary to sacrifice determinacy in the load path by adding redundant non-conforming contacts for some degrees of restraint (DOR) to meet our minimum stiffness requirements.

Having a hinge as part of the deployed load path of a precision deployment mechanism adds complexity and uncertainty. Using a loose hinge pin that controls deployment but takes the hinge out of the latched load path can alleviate the uncertainty while minimizing complexity. We found this to be the case for the PM wing latches. However, we found the benefits of this approach to be application specific and felt that the SMSS mid-hinge design was better with the hinge designed as part of the deployed load path.

In other instances it was difficult to have semi-kinematic or non-conforming interfaces and the loads needed to be taken by friction joints. This was the case for the SMSS end-hinges. To compensate, the load capacity (i.e., stick-slip load) of the interface was designed per the recommendation of [1], to be much greater (e.g., a factor of 10 greater) than the maximum expected operating load of the mechanism.

In all applications the deployment mechanisms were located in-line with the primary load carrying members of the structure and the footprint of the latches was maximized to minimize the sensitivity to instabilities at the latch interfaces. In addition, the stiffness of the latches was maximized by minimizing their effective length and maximizing the elastic stiffness with high-modulus materials (e.g., titanium). This also proved to be beneficial for thermal stability since it minimized the length of the higher CTE materials.

Distributed preload systems were used in most applications since it was not practical from a mass and cost standpoint to have an independent preload device for each latch interface. However, the preload mechanisms were designed to be much more compliant than the interface fittings which transfer the operational loads. Providing this compliance keeps the preload device out of the primary stiffness path and maintains a relatively constant preload across the interfaces.

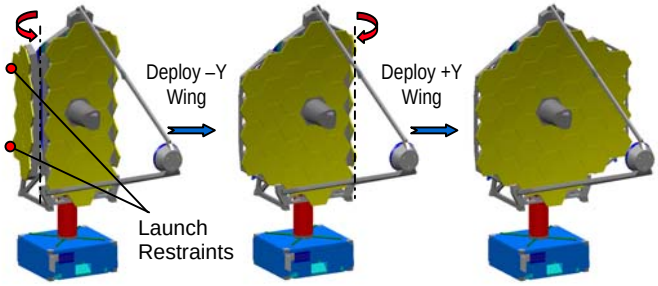

Figure 5. Primary Mirror Wing Deployment

Primary Mirror

The primary mirror deployment and latch mechanisms consist of a pair of hinges and four latches for each wing. The deployment hinges and wing latches act as independent systems.

Wing Deployment Hinges

The hinges have a dual function. First, the hinges, along with two launch restraint mechanisms, carry the wing launch loads. Second, they rotate the wings 103 degrees into the capture range of the deployed wing latches. The wing deployment sequence is shown in Figure 5. Each hinge has a pair of lug and clevis fittings joined by a loose hinge pin providing redundant rotating surfaces. The hinge pin has sufficient clearance to the lug and clevis fittings to preclude it from being in the load path after the latches have been secured. This guarantees the hinges will not affect deployment repeatability or generate loads during operation that could cause micro-dynamic instabilities at the critical latch interface.

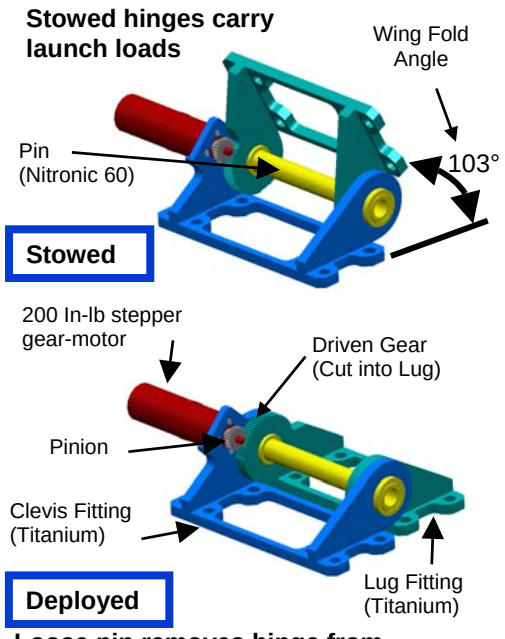

Figure 6. Deployment Hinge Design Details

A stepper gear-motor mounted to the lug of one of

the two deployment hinges is used to rotate the wing from the stowed to the deployed position. The gear-motor drives the clevis fitting through spur gears that provide a 4/1 gear ratio over the motors 22.5 Nm (200 in-lb) output torque capability for roughly 90 Nm (800 in-lb) of available deployment torque. The hinge fittings are machined out of titanium and the hinge pins are Nitronic 60 to prevent galling. The bolt hole pattern on the titanium fittings has a single pinned hole along with oversized and slotted holes to allow the fittings to shrink with respect to the near zero CTE composite backplane structure. MoS_2 dry film lubricant is used on the hinge gears, hinge pins, and the spacers between the lug and clevis ears. The details of the hinge design are shown in Figure 6.

Wing Latches

The latches have a singular role and are not in the load path during launch. Their function is to align and secure the deployed backplane wings to the backplane center section, thus creating the stable backplane structure that supports the 36 primary mirror segments. The driving requirements for the wing latch design were deployment repeatability, deployed stiffness (to meet LOS and WFE jitter requirements), thermal stability and micro dynamic stability.

We believed the best way to achieve good wing deployment repeatability was to use a kinematic interface with fittings specific to the six degrees of restraint (DOR). The six DOR are implemented at three locations across the interface between each wing and the backplane center section. At the first location a 3-DOR latch set provides a sphere-in-cup interface that locates the wing in the two in-plane directions and provides one of the three points that defines the interface plane. The second location holds a 2-DOR latch set that provides a sphere in groove interface that fixes the rotation about the first fitting set and establishes the second point of the interface plane. The third location holds a 1-DOR latch set that is a sphere on a flat and is the final point needed to define the latch interface plane. The latches are shown in Figure 7. They are lubricated with MoS_2 for low friction between the mating pairs and to prevent cold welding, and a 2669-N (60-lb) preload is used to drive the fittings into the same determinate position each time.

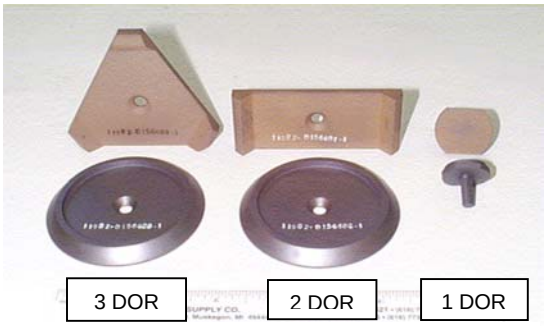

Figure 7. Latch Sets

Because the wing to center section is long and slender, it wasn't possible to provide the deployed wing natural frequency required for LOS and WFE jitter with just three fitting sets. Therefore, five adjustable non-conforming 1-DOR (A1 Fittings) sets were added and configured in pairs as shown in Figure 8 with a cryogenic preload device centered between each pair. The pairs of fittings were located as far apart as possible using the entire depth of the backplane to provide the largest footprint and most efficient stiffness path.

The latch sets, shown in Figure 7, are Ti 6Al-4V ELI. More exotic, lower coefficient of thermal expansion (CTE) materials such as silicon carbide were considered for the latch materials. However, these materials would have been very costly. By keeping the cross sections of the latches thin, this common, robust metallic could be used while maintaining overall thermal distortions to well within the allocation. The final latch design was 12.7-mm (0.5") thick (shown in Figure 9).

To eliminate loads at the latch interface due to thermal cool-down, cryogenic preload devices are engaged and only lightly loaded during the initial deployment. Then, after the OTE has cooled to its final operating temperature, the devices are backed off to remove any stresses in the system. Finally, the latch sets are preloaded again to their flight operational levels.

To keep the Hertzian stresses low on the titanium latch sets with a 2669-N (600-lbf) preload, a 100-mm (~4") radius was required on the spherical half of the set. This was easy to accomplish with the 1-DOR latch set that consisted of a spherical fitting interfacing with a flat. It was slightly more difficult for the 2-DOR and 3-DOR latch sets since it was desirable for the spherical surfaces to interface with flats at a 45° angle to provide similar stabilizing forces in the axial and transverse directions. The limits of 12.7 mm

(0.5”) thickness, 100-mm (4”) spherical radius and 45° interface flats drove the resulting geometry. Since the resulting fittings had a diameter of 83 mm (3.25”), the fittings had to be installed with a single fastener centered on the fitting so that positioning was maintained, and the CTE mismatch between the fittings and the near-zero CTE backplane structure would not result in unacceptably high loads.

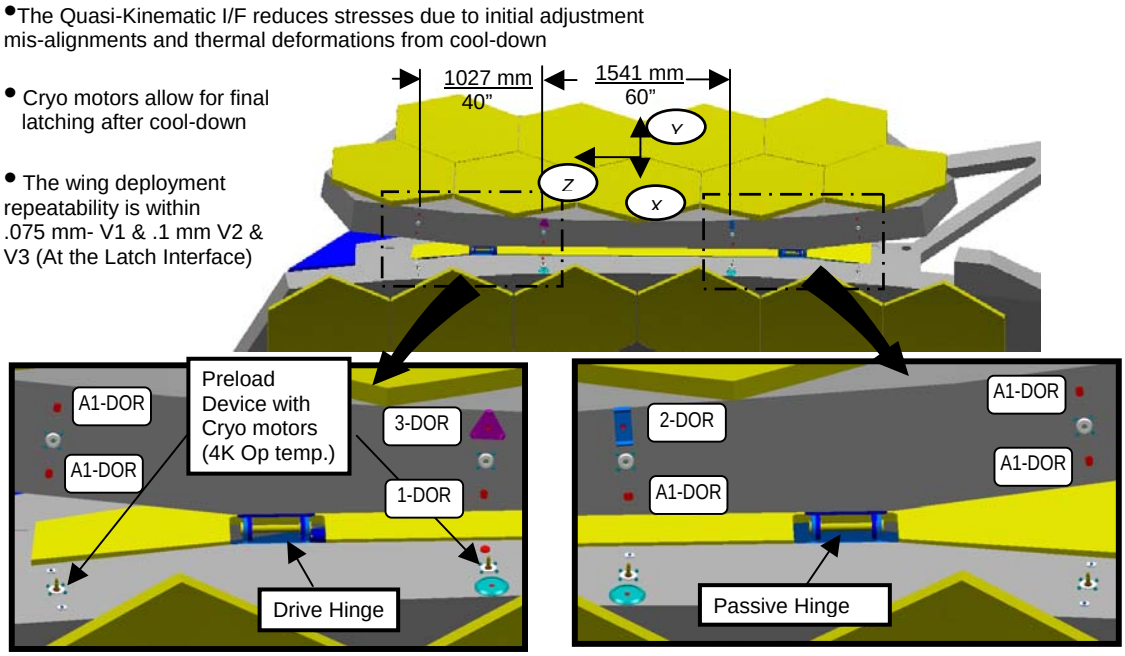

Figure 8. Primary Mirror Hinge and Latch Sets

The preload device for the latches uses a 3/8-24 UNJF-3A screw driven by a stepper gear-motor that engages and screws into a floating nut in the mating latch (Figure 10). The two halves of the device are pulled toward each other but never bottom out so the preload device never provides a stiff load path. It is critical to have the nut properly aligned to the drive screw before it starts turning to prevent cross threading. The floating nut is spring loaded in a loose housing that prevents nut rotation during tightening but allows a small amount of angular motion for nut to drive screw alignment during engagement. A feature was also added to the tip of the drive screw to guide the nut onto the screw and prevents the nut from rotating the mating threads out of alignment. The screw material is A286 CRES chosen for its high strength, and Nitronic 60 was chosen for the mating nut for its anti-galling characteristics. To minimize the torque resistance to the gear-motor, the drive screw has MoS_2 lubrication and a thrust bearing was used between the base of the drive screw and its housing. The thrust bearing also provides a desired compliant element to the preload device.

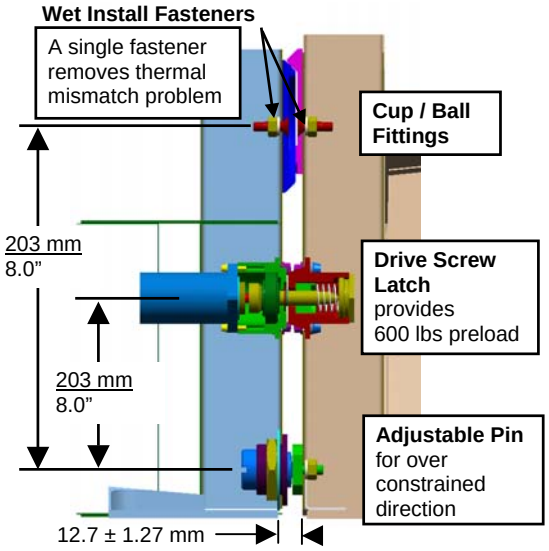

Figure 9. Latch Design Details

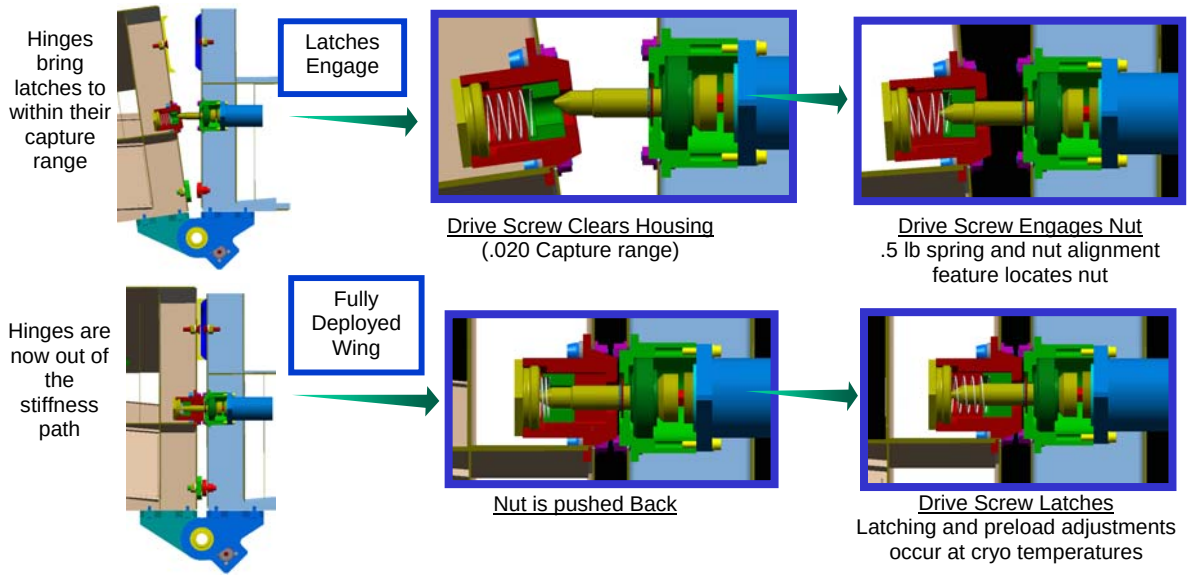

Figure 10. Wing Latch Engagement and Preload

Secondary Mirror Support Structure

The SMSS design is a deployed tripod as shown in Figure 11. A tripod design was selected because of its superior dynamic stability and mass efficiency. The deployment system is a four-bar linkage driven by a stepper gear-motor. Since wavefront error (WFE) is very strongly affected by axial despace (defocus) of the secondary mirror assembly (SMA), the design uses a very low CTE composite material system in the SMSS tubes. This produces a very small despace contribution to wave front error over the worst-case hot-to-cold conditions.

SMSS Deployment Drive

The SMSS is driven by a single stepper gear-motor located at the inboard single strut hinge as shown in Figure 12. This hinge was selected as the drive location since it provides the best mechanical advantage for the system. The gear-motor pinion drives a spur gear mounted on the inboard single strut providing an additional 4/1 gear ratio over the 22.5 Nm (200 in-lb) torque capability of the gear-motor. This provides roughly 90 Nm (800 in-lb) of drive torque capability.

The SMSS, like the PM wings, is configured to minimize stresses in the system while latching. Although all five SMSS hinges are latched, the mid-hinge is the only one to be preloaded into hard stops. Because

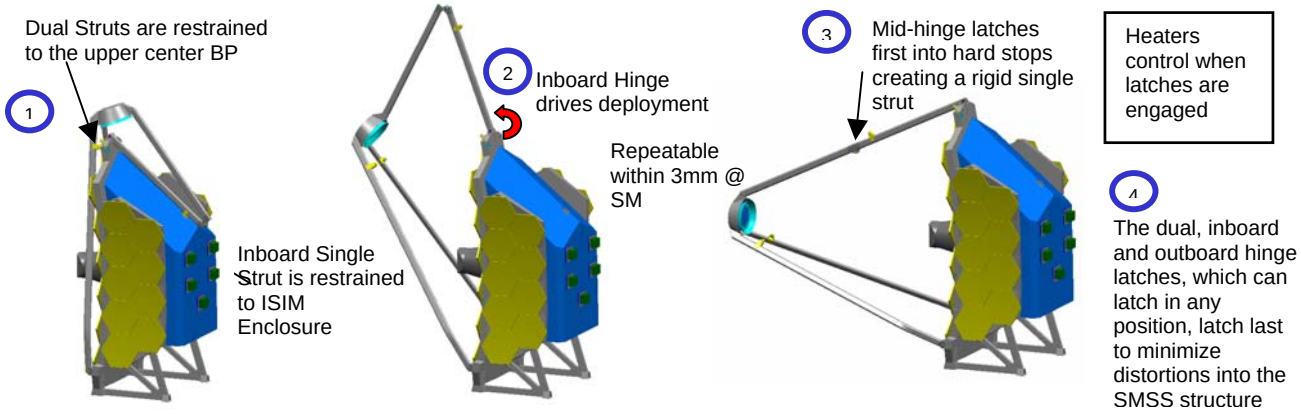

Figure 11. Secondary Mirror Support Structure

the four remaining latches take advantage of the thermal shrinkage of their aluminum components to clamp them in place during cooldown to operating temperature, they can latch at any angle of rotation.

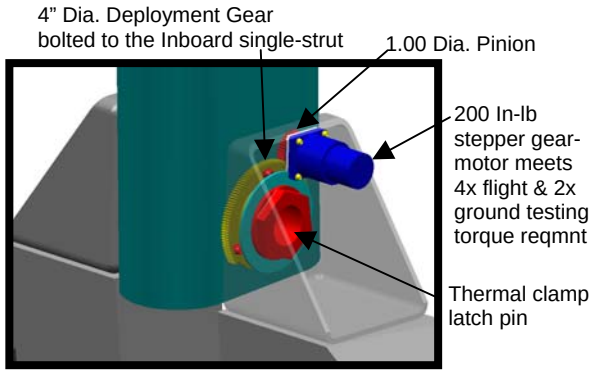

Figure 12: SMSS Deployment Drive

SMSS Mid-hinge

The mid-hinge is deployed through a 168-degree rotation and bottoms out on hard stops at the end of its travel. There are two leaf spring latches (one on each side of the hinge) that engage at this point capturing catch fittings on the mating hinge half. The catch and latch base fittings are machined titanium and the leaf-spring latch is 7075 Aluminum. The latches are centered on the hinge (Figure 13), so that as the temperature drops from RT down to ~30K, the aluminum latches shrink and preload the M55J composite hinge at its two adjustable hard stops and two hinge pin to bushing interfaces. The stops provide non-conforming sphere-on-flat interfaces and the pin bushings are notched to provide non-conforming line contact interfaces.

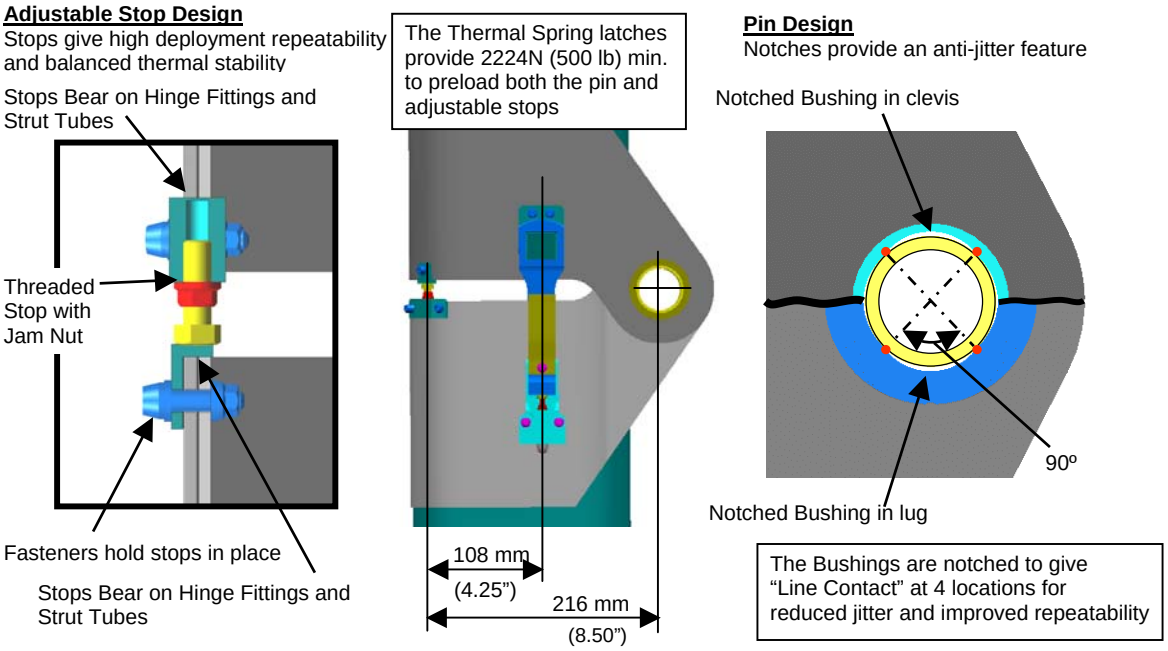

Figure 13. Mid-hinge Latches and Hard Stops

A spring feature was added to the latch to help compensate for any creep that could occur over the life of the mission and help provide a well-defined stiffness path. The stack of Bellville washers, shown in Figure 14, is roughly half the stiffness of the aluminum latch and has a 1-mm (0.040") stroke. Two stops were required to meet the natural frequency requirement of the hinge, and the process for adjusting them to get an equal load distribution has been demonstrated on the DOTA hardware.

SMSS End-hinge

The end hinge design is common to the dual strut hinges and the inboard and outboard single strut hinges. It has a rotation pin that provides precision deployment location plus a clamping pin that preloads the lug and clevis bushings together once the hinges are in their final deployed locations. The latches will

latch in any position without forcing the hinge to a preset location and provides a 10x load carrying capability over operational loading. The end hinge design details are shown in Figure 15.

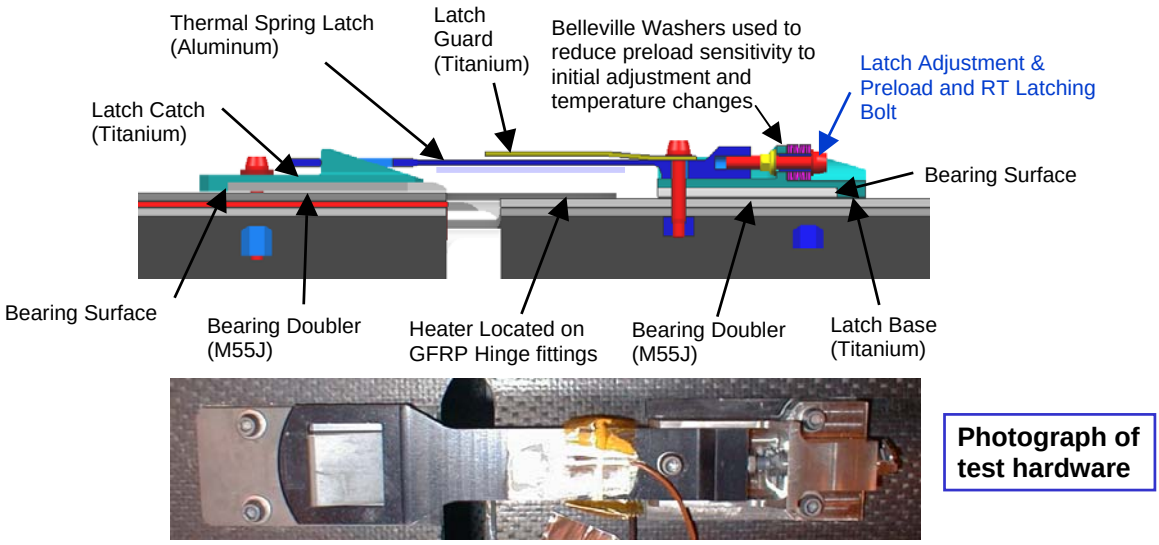

Figure 14. Mid-hinge Preload Mechanism

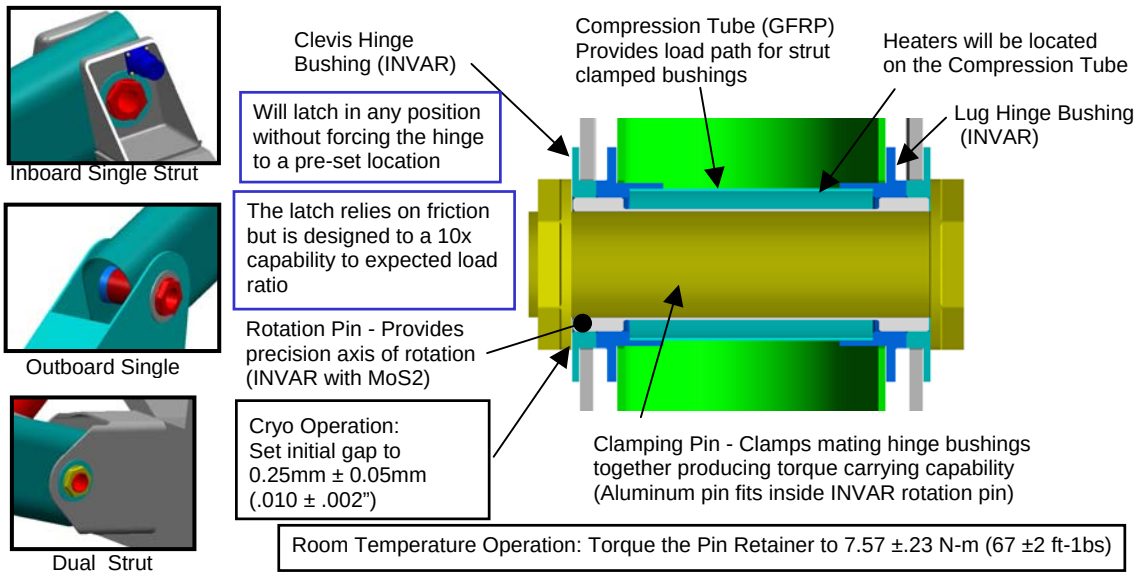

Figure 15. End Hinge Latch Design

Deployment Repeatability

The deployment repeatability of the SMSS must be such that once the latches are engaged and preloaded, the secondary mirror is within the wavefront capture range of the wavefront sensing and control system (WFS&C). The tripod design is a geometrically robust design for locating the SMA within the allowable capture range and is driven primarily by the size of the gap between the end hinge pins and bushings. The repeatability requirement and analysis result are shown in Table 5.

Table 5. SMSS Deployment Repeatability

	X Despace (mm)	Y Decenter (mm)	Z Decenter (mm)	Theta Z (arcmin)
Requirement	3	3	3	1
Analysis Result	< 1	< .5	< .5	< .5

Development Testing

This section covers the DOTA testing and associated results including; deployment capability and measurements of the repeatability of the PM wing mechanisms, characterization of the micro-dynamic stability of the wing latching system, functional latching of the SMSS hinge latches, and measurement of the load carrying capability of the SMSS end hinge. Details of the test metrology and procedures and additional thermal stability results can be found in [2].

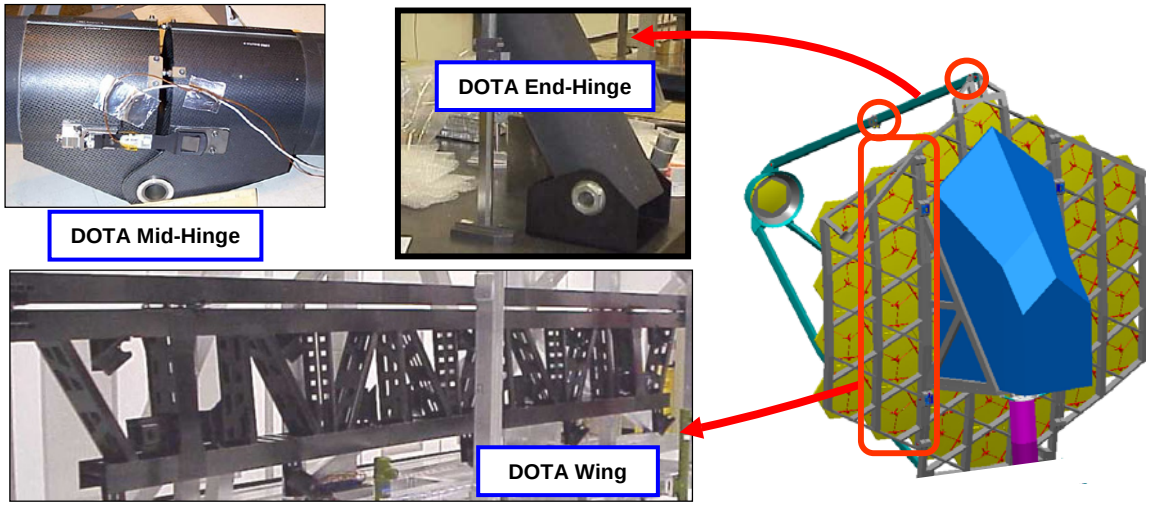

Figure 16. Cryogenic Development Optical Telescope Assembly (DOTA)

In order to understand the behavior and reduce the risk associated with very large, deployed optics support structures, NGST developed and tested the DOTA PM wing and SMSS hinges. The DOTA wing replicates a full-scale portion of the JWST PM support structure and includes a hinge-line with a full set of latches so the overall stability of the system can be characterized. The DOTA SMSS hinges and latches replicate full-scale end and mid-hinges. The DOTA hardware is shown in Figure 16.

The DOTA wing hinge/latch testing was broken into two parts. The first part had the hinges and latches integrated into an aluminum test fixture that simulated the flight structure. They were then tested as a unit at room temperature (RT) for deployment repeatability and micro-dynamic stability. Once this testing was complete, the mechanisms were removed from the test fixture and integrated onto the DOTA wing structure. Then, as an integrated structure, the DOTA wing was tested at cryogenic temperatures for thermal and micro-dynamic stability.

Hinge/latch repeatability

The fixture that the wing hinges and latches were tested on is shown in Figure 17. The hinge-line was scaled down in the Z direction to facilitate testing. The deployment repeatability requirements are derived from the JWST need to have the Primary Mirror within the capture range of the WFS&C system. Deployment repeatability was measured in X, Y, Z and Theta Z directions. For each test, the hinge was driven 103 degrees from the stowed to the deployed position using a flight-like stepper gear-motor. The latches were then engaged using a torque wrench to accurately assess the torque being applied. The test was repeated 10 times for both a 1.13 Nm (10 in-lb) latching torque and the 11.25 Nm (100 in-lb) latching

torque. Repeatability measurement results are given in Table 6. The latch repeatability tests demonstrate that the DOTA wing latches easily meet the repeatability requirements for wavefront capture. The repeatability tended to degrade with higher preload and we believe this was due to the lack of stiffness in the aluminum test fixture. Although the test data met all the requirements with margin, even smaller repeatability errors are expected with the stiffer flight backplane.

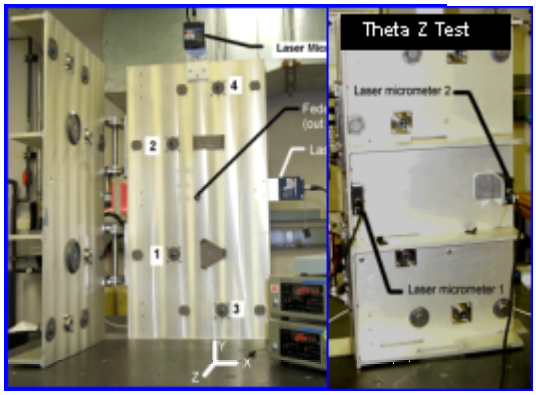

Figure 17. Test Configurations for Repeatability Measurements.

Table 6. Deployment and latching repeatability results, one-sigma

	X Despace (mm)	Y Decenter (mm)	Z Decenter (mm)	Theta Z (arcmin)
1.13 Nm error	0.020	0.030	0.043	0.15
11.25 Nm error	0.033	0.043	0.030	0.74
Requirement	1	0.1	0.1	1.0

Latch Micro-dynamic Testing

Over 100 load cycles were applied during the RT micro-dynamic testing of the DOTA latches with shear and moment loads significantly higher than those expected operationally. The first set of tests applied cyclical quasi-static loading at 0.1 Hz in each shear direction. Since it's believed that the micro-dynamics in a deployable structure is related to hysteretic response, the displacements were measured in all three directions and the hysteresis was determined by removing the linear response. Sample hysteresis results are shown in Figure 19.

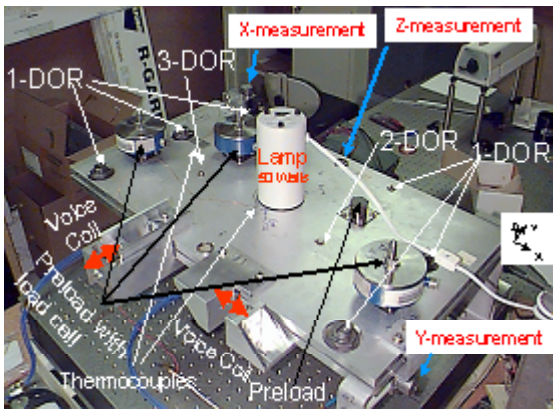

Figure 18: μ-dynamics Testing

The next set of testing also applied cyclical loading to the latch interface, while looking for evidence of "nanolurches". Sample results for this testing are shown in Figure 20. The 9-nm lurch shown occurred with the latches at half of the operational preload and with an applied load 100 times operation loading. The final set of tests run with this latch micro-dynamic test setup applied a thermo-elastic load across the latched interface 10,000x greater than the operational thermo-elastic load. The series of tests revealed no evidence of "nanolurches" when the preload applied to the latch was consistent with its operational design of 2669 N (600 lb). Moreover, only 3 nanolurches were detected during all of the testing, with these occurring when latch preloads of 1334.5 N (300 lb) or less were applied.

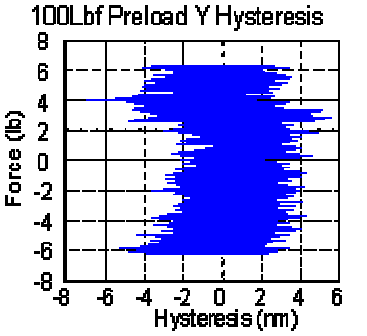

Figure 19. Sample Hysteresis Test

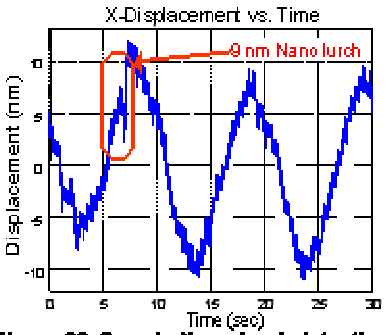

Figure 20. Sample Nano-lurch detection

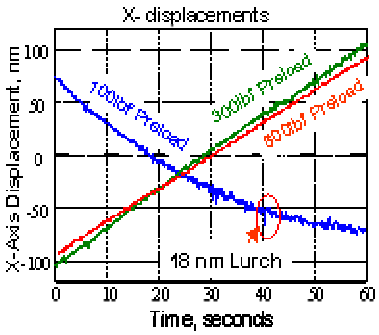

Figure 21. Sample μdynamic Thermal Test

Thermal Stability Testing

After the latch testing was completed, the latches were integrated onto the DOTA wing structure. The DOTA wing was then transported to the Marshall Space Flight Center in Huntsville, Alabama for thermal stability testing down to cryogenic temperatures in the X-Ray Calibration Facility. Figure 22 illustrates how distance-measuring interferometers were configured to monitor the latch interface at several locations along the hinge-line. Similar to the micro-dynamics testing discussed previously, the interferometers were used to look for discontinuities in the latch behavior.

The interferometers detected frequent slips as the DOTA first achieved temperature, as depicted in Figure 23. Three of the four latches were powered for the DOTA testing and these latches were released and re-tightened (Figure 24) as planned after cool-down. As expected, this significantly reduced the amplitude and frequency of the slips. Bulk temperature testing and gradient testing was then performed on the DOTA. The bulk temperature testing consisted of a 20K thermal excursion. This was 100 times larger than the expected on-orbit thermal excursion of 0.2K creating 100x the thermal loading in the latch interface. Moreover, the gradient testing far exceeded this multiplier compared to on-orbit expectations.

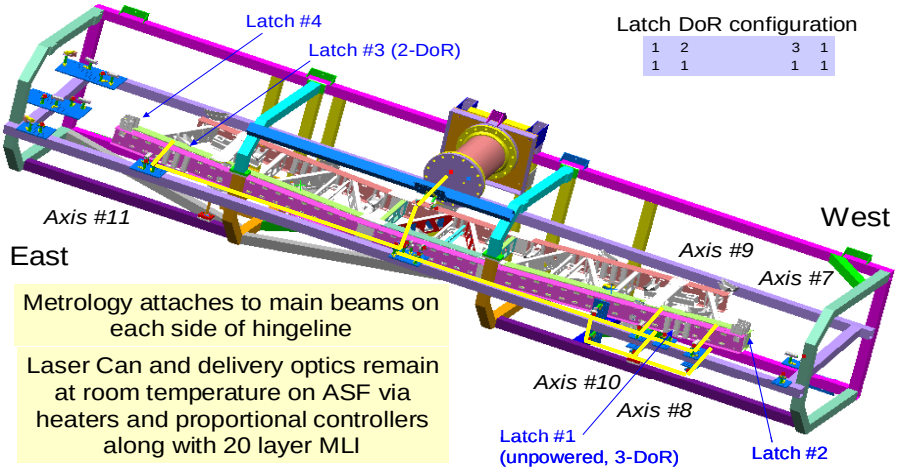

Figure 22. DOTA Hinge-line Metrology Beam Paths

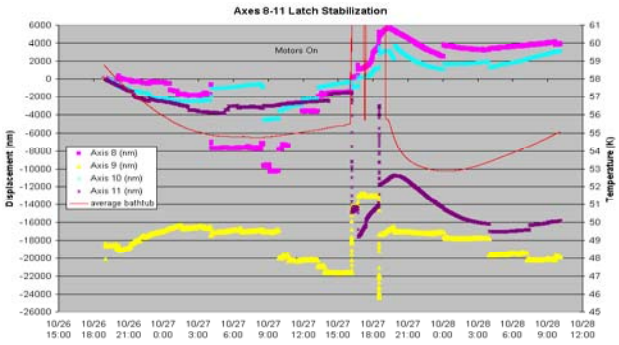

Figure 23. Hinge-line Displacements at the End of the Cool-down

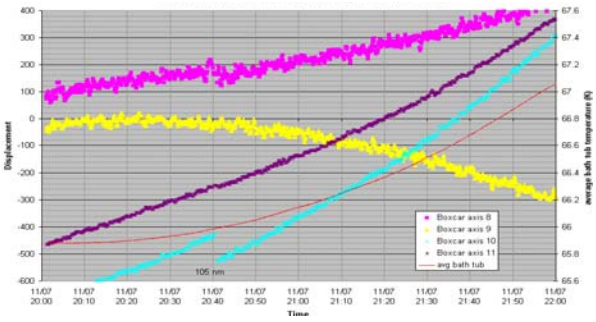

Figure 24. Latch Interferometer Data During Bulk Temperature Test

Under these high loads, interferometer axis 10 exhibited stick-slip behavior in two instances, with no other measurable discontinuities in the data. Without the ability to re-torque this latch, it suffered the loss in pre-load that results from cooling from room temperature to 50K. The observed slippage at the latch with the lower preload that is absent at the latches with operational preloads correlates with the room temperature micro-dynamic performance measurements.

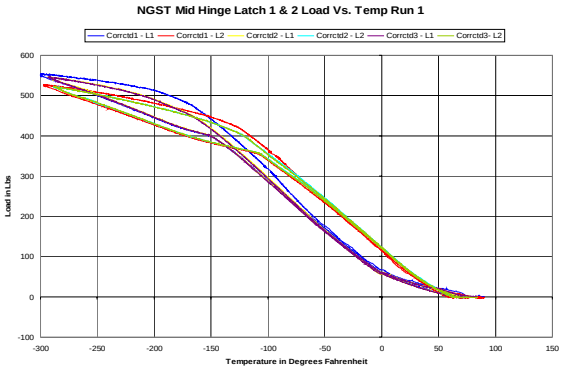

Figure 26. SMSS Mid-hinge Load vs. Temp

DOTA SMSS Hinge / Latch Testing

To verify the key components of the SMSS, a prototype of each type of hinge (i.e., a mid-hinge and an end hinge) was built and tested. The purpose of the testing was to verify functional latching at cryogenic temperatures. In addition, the end hinge was tested to show that it has a minimum 10x margin against operational loads. Micro-dynamic stability testing on the hinges is also planned for early 2005.

The cold box shown in Figure 25 was used to take the hinges down to ~88K using LN_2. Flight temperatures of ~20K could have been reached using liquid helium; however, the added expense couldn't be justified given that flight preloads were achieved at the higher LN_2 temperatures by simply adjusting the initial latch gaps accordingly.

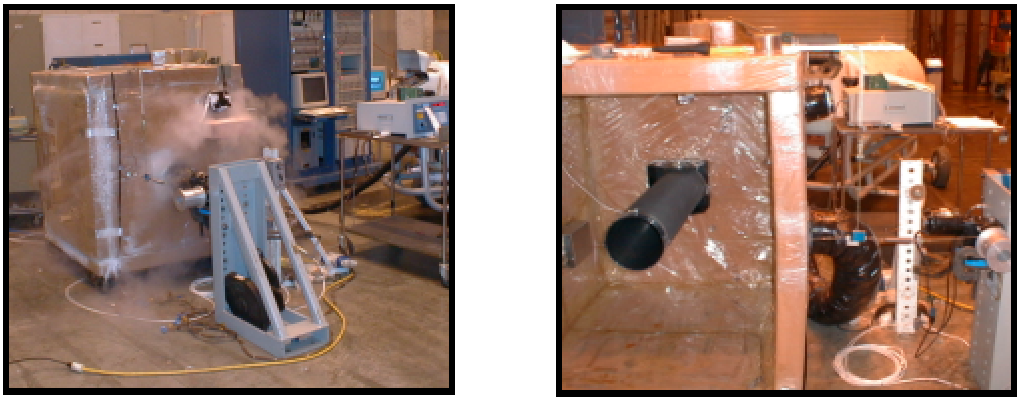

Figure 25. SMSS Hinge Testing

Mid-hinge Testing

To test the Mid-hinge thermal latches, the preload in the spring latches needed to be monitored as the hinge assembly was taken to cryogenic temperatures. The two aluminum spring latches were instrumented with thermistors and strain gages that were calibrated down to 80K. The latch gap between the spring latch and the catch was set for a desired preload of 2335 N $\pm$ 111 N (525 lb $\pm$ 25 lb). The latches were then cycled down to ~88K (-300°F) and back to room temperature 3 times to characterize any creep due to loading and unloading the assembly. The results of the testing in the form of preload verses temperature curves are shown in Figure 26.

Several things were apparent from the test results that will help in the design of the flight latches. First, the latches proved to be very repeatable with the cool-down curves for the three cycles lying nearly on top of each other. Also, the stiffness of the latch preload paths for latch 1 & 2 were very well matched, but only after the initial cool-down from room temperature to ~255K (0°F). The Bellville washer stacks demonstrated good repeatability and well matched stiffness during cool-down, but the non-linear behavior and large amounts of hysteresis that is often associated with Bellville washers was evident as the latches warmed back up to room temperature.

In addition to setting the initial gap of the latches, the preload in the Bellville washer stacks is set to just below the desired operational preload. This was accomplished for the DOTA testing by measuring the desired compression of the washer stack by counting turns on the preload nut. Since this method lacked precision, the resulting initial preloads of latch 1 & 2 were off by roughly 445 N and 663 N (100 lb and 140 lb) respectively. This, however, was balanced by the added compliance in latch 1 and both latches achieved the desired flight preload.

The Bellville washers served their purpose for the DOTA test and demonstrated the advantage of having a compliant member in the latch stiffness path. However, we are currently looking into replacing the Bellville washers with a machined spring in order to increase the compliance, further reducing the sensitivity to thermal changes, and to reduce the non-linearity of the latch.

End Hinge Testing

The end hinge DOTA testing was very similar to the mid-hinge test. The clamping pin was instrumented with thermistors and a strain gage and taken down to 88K. The hinge was cycled 5 times and demonstrated very good repeatability as shown in Figure 27.

In addition, a cable with a spring and a load cell was attached to the end of the end hinge strut and tensioned with a motor until the latch broke loose. An LVDT was used to measure displacements of the strut near the latch and clearly indicated when the torque generated by the motor exceeded the torque carrying capability of the latch. The test was repeated 3 times at six temperatures (preloads), and as expected, proved to be very repeatable. The results are plotted in Figure 28 as applied slip force verses latch preload. The flight preload of 13,345 N (3000 lbf) provided an 8.47 N-m (75 in-lb) torque carrying capability, which is 10x greater that the expected on-orbit loads.

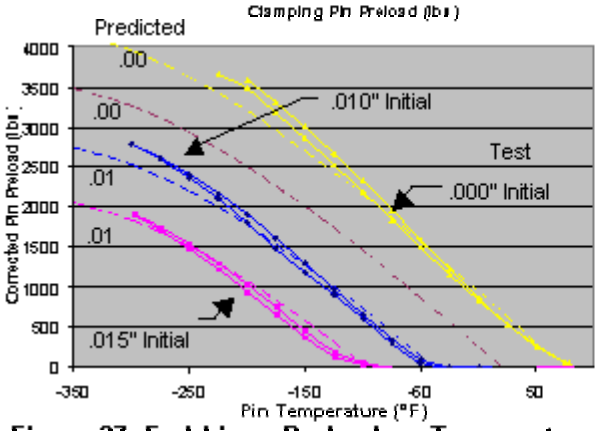

Figure 27. End-hinge Preload vs. Temperature

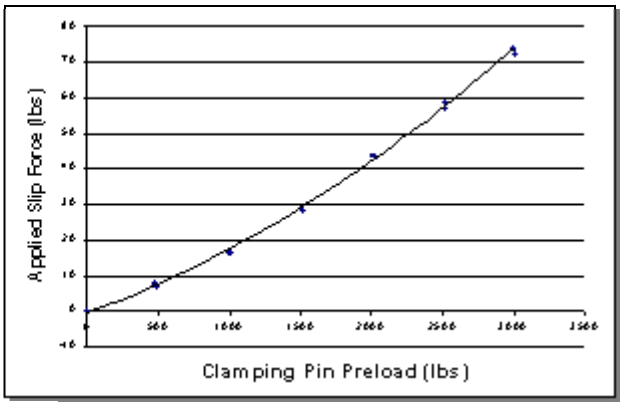

Figure 28. SMSS End-hinge Force vs. Preload Plot

Concluding Remarks

The observatory architecture and design details described in this paper are a “point in time” design that was submitted as part of the Phase 2 JWST proposal in October 2001. The program had a replan exercise in an effort to reduce program cost. This replan effort resulted in several significant changes to the architecture including a reduction in the PM diameter from 7 m to 6.5 m and a change to the number of segments in the primary mirror from 36 to 18. These architecture changes have resulted in some small impacts to the designs described in this paper, but essentially, the designs have stayed the same. As a result of the DOTA early development testing, the OTE’s primary deployment system designs have been shown to satisfy their driving requirements. Consequently, this testing has proven to be very effective in reducing the program risk associated with these optically stable deployable structures.

References

1. Lake, Mark S. and Hachkowski, M. Roman. “Design of Mechanisms for Deployable, Optical Instruments: Guidelines for Reducing Hysteresis.” NASA/TM-2000-210089, (March 2000)
2. Atkinson, Charlie, Gilman, Larry and Reynolds, Paul. “Technology Development for Deployable Telescope Structures and Mechanisms.” SPIE Conference Paper 4850-45 (June 2002)